Field Testing of LIDAR-Assisted Feedforward Control Algorithms for Improved Speed Control and Fatigue Load Reduction on a 600-kW Wind Turbine

Preprint

Avishek A. Kumar and Ervin A. Bossanyi
DNV-GL

Andrew K. Scholbrock and Paul Fleming
National Renewable Energy Laboratory

Mathieu Boquet and Raghu Krishnamurthy
Leosphere-Avent

NOTICE

Field Testing of LIDAR Assisted Feedforward Control Algorithms for Improved Speed Control and Fatigue Load Reduction on a 600 kW Wind Turbine

Avishek A. Kumar, Ervin A. Bossanyi, Andrew K. Scholbrock, Paul A. Fleming, Matthieu Boquet, Raghu Krishnamurthy

Abstract

A severe challenge in controlling wind turbines is ensuring controller performance in the presence of a stochastic and unknown wind field, relying on the response of the turbine to generate control actions. Recent technologies such as LIDAR, allow sensing of the wind field before it reaches the rotor.

In this work a field-testing campaign to test LIDAR Assisted Control (LAC) has been undertaken on a 600-kW turbine using a fixed, five-beam LIDAR system. The campaign compared the performance of a baseline controller to four LACs with progressively lower levels of feedback using 35 hours of collected data.

The collected data indicates that utilising measurements from multiple range gates on a pulsed LIDAR system can result in rotor averaged wind speed (RAWS) estimates with greater levels of correlation with wind speed at the rotor than using a single range gate. The LACs showed higher levels of speed control performance with significantly reduced levels of pitch activity and generally lower levels of tower excitation. Although the loading spectrum for the test turbine was dominated by responses at twice the rotor speed (2P) and the first tower fore-aft natural frequency, the reduction is likely to show greater relative significance on typical full-sized turbines, which show lower excitation levels due to harmonic clashes.

A. A. Kumar is a Control Engineer with DNV GL - Energy, Auckland, New Zealand (phone: +64-9-414-5572; fax: +64-9-414-5573; e-mail: avishek.kumar@dnvgl.com).

E. A. Bossanyi is a Senior Principal Researcher with DNV GL - Energy, Bristol, UK (phone: +44-203-816-4270; e-mail: ervin.bossanyi@dnvgl.com).

A. K. Scholbrock is a Field Test Engineer at the National Wind Technology Center, Golden, CO 80401, USA (phone: +1-303-384-7181; fax: +1-303-384-6950 ; e-mail: andrew.scholbrock@nrel.gov).

P. A. Fleming is a Senior Engineer at the National Wind Technology Center, Golden, CO 80401, USA (phone: +1-303-384-7181; fax: +1-303-384-6918 ; e-mail: paul.fleming@nrel.gov).

M. Boquet is Lead of Science and Application at Leosphere-Avent, Paris, France (e-mail: mboquet@leosphere.com).

R. Krishnamurthy a Science and Application Engineer at Leosphere-Avent, Paris, France (e-mail: rkrishnamurthy@leosphere-avent.com).

I. Introduction

A severe challenge in controlling wind turbines is ensuring controller performance in the presence of a stochastic and unknown wind field, relying on the response of the turbine to generate control actions. Recent technologies such as LIDAR, allow sensing of the wind field before it reaches the rotor. This information allows controllers to work in an anticipatory mode, potentially improving control performance [1] and leading to reduced costs of energy through load reduction and reduced actuator usage.

A number of methods have been researched using simulation studies to exploit preview wind information ranging from basic [2] and advanced [3]–[5] feedforward algorithms to model predictive control methods [6]–[8]. Although most methods have been tested in simulation on models of various fidelity, feedforward controllers have begun to be field tested on full-scale turbines [9]–[11].

In this work we present the results of field testing a feedforward control algorithm that utilises LIDAR measurements on a full-scale wind turbine. This work contributes the first set of public field tests of a feedforward controller in conjunction with a five-beam pulsed LIDAR system. This paper makes use of approximately 35 hours of data in a range of wind conditions and multiple controller tunings to show the impact on rotor speed control, pitch actuator usage and tower loading from LAC.

II. Approach

A. CART2 Wind Turbine

Testing has been conducted on the Controls Advanced Research Turbine (CART2) wind turbine at the National Wind Technology Center in Colorado, USA. The CART2, a two-bladed variable-speed, variable-pitch turbine with a 42.7-m rotor diameter [2], is nominally rated at 600 kW, however, for the purposes of this study, the turbine has been de-rated to 128 kW to maximise the time during which pitch control is active because the measurements took place during a period of low wind speeds. The resulting set points for rated rotor speed, generator speed and generator torque were set at 24 rpm, 1036 rpm and 1182 Nm, respectively.

B. LIDAR System

The preview wind information used for control was obtained by a nacelle-mounted LIDAR system created by Avent LIDAR Technology. The Avent five-beam LIDAR unit uses a pulsed LIDAR with five fixed beams, each capable of sampling the line-of-sight (LOS) wind speed at up to 10 ranges simultaneously. The LIDAR is mounted on the nacelle facing upwind, as shown schematically in Fig. 1 and on-site in Fig.2. The LIDAR also processes the LOS data to return the current RAWS estimate, wind shear estimate and wind direction estimate for each range gate. The RAWS is defined as the mean wind speed over the rotor swept area at a defined plane (not necessarily at the rotor).

For the purposes of this testing campaign, the feedforward control algorithm makes use of the RAWS data from three range gates focused at 50 m, 65 m and 80 m. These gates correspond to covering the centre and approximately 63%-100% of the rotor radius using a beam angle of 15° from horizontal.
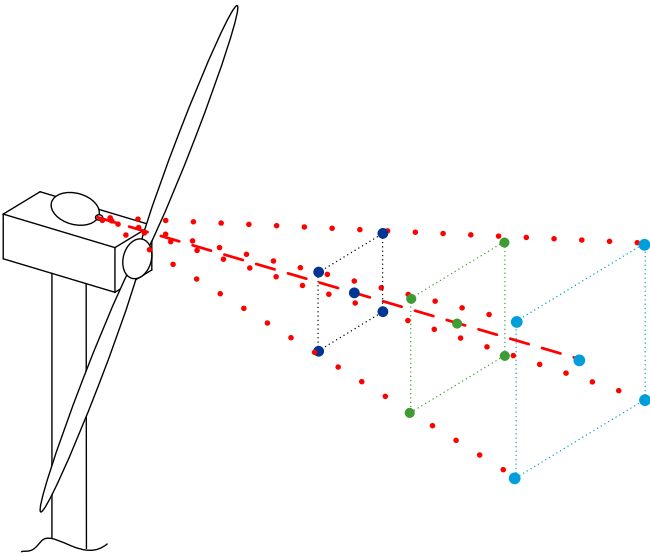

Figure 1. LIDAR mounting and scanning schematic. Red lines indicate LIDAR beams, green dots indicate scan points, dashed lines indicate orientation axis and dash-dot lines indicate range gate plane.

C. Baseline Feedback Controller

The CART2 was de-rated to have a rated wind speed of 8 ms^{-1} (128-kW rated power) in order to function in the pitch control regime as much as possible for this study. The CART2 has separate generator torque and blade pitch controllers to maintain the required rotor speed. The generator torque is applied as a function of filtered generator speed, attempting to track the optimal power coefficient until the rotor speed is 19.2 rpm, after which the torque is

Figure 2. Avent five-beam LIDAR sytem mounted on the CART2. (Photo Credit: Lee Jay Fingersh, NREL 33621.)

increased linearly until it saturates at 1182 Nm coinciding with a rotor speed of 22.9 rpm. The pitch controller becomes active to regulate the rotor speed to 24 rpm once the turbine reaches maximum torque. This speed is obtained at wind speeds of approximately 8 ms^{-1}. The controller is implemented as a gain-scheduled PI controller using the filtered generator speed as feedback, typical of full-scale wind turbines.

D. Feedforward Controller

The feedforward controller is designed to use preview wind measurements to assist the feedback controller in speed control, with the aim of achieving higher levels of speed control performance and/or reduced levels of pitch activity. We approximate the entire wind disturbance acting on the rotor by a RAWS at the rotor plane (V) and focus on rejecting low frequency aspects of the disturbance. We can then apply a static control law based on the steady-state blade pitch as a function of RAWS. This method has been shown to be successful at reducing rotor speed variance in both field testing and simulation [9], [10]. The control law moves the pitch actuators pre-emptively to the correct steady-state pitch angle for the incoming wind field through the following algorithm:

$$\dot{\theta}_{FF}(t) = \frac{\hat{\theta}_{ss}(V(t+\tau)) - \hat{\theta}_{ss}(V(t))}{\tau} ,$$

where $\dot{\theta}_{FF}$ is the feedforward pitch rate, $\hat{\theta}_{ss}$ is the steady-state pitch angle for a given wind speed and τ is the look-ahead time (LAT). The feedforward control signal is then added to the feedback signal as shown in Fig. 3.

The LIDAR system used for this study provides an estimate of the RAWS at three range gates $V(t+\tau+T)$, where T is the time-to-rotor (TTR) determined by:
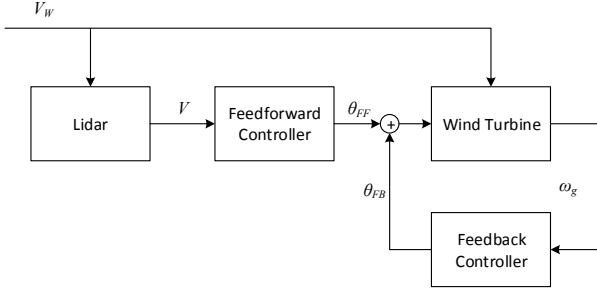
$$T = \frac{D_i}{V_c} - \varepsilon ,$$

Figure 3. Schematic of pitch control architecture. V_w is the wind field, V is the LIDAR-estimated RAWS data, θ_{FF} is the feedforward pitch angle, θ_{FB} is the feedback pitch angle and ω_g is the generator speed.

where D_i is the distance between the rotor plane and the focus plane of range gate i, V_c is the convection speed and ε represents any processing delays. The convection speed is determined by low-pass filtering $V(t+\tau)$. The TTR decreases on each controller time step and when a RAWS estimate has a TTR equalling the LAT or has reached the rotor (TTR of 0) it is low-pass filtered (to avoid discontinuities caused by combining data from multiple range gates) and used in the feedforward algorithm.

III. Results

To analyse the control performance, the CART2 was run in a de-rated state, cycling between LAC and Baseline control every 5 minutes. Data was binned into contiguous 45-second samples in which the minimum rotor speed was above 23 rpm (96% rated) and the minimum generator torque was 1000 Nm, both indicating above-rated operation with pitch action. The sample length choice was based on a trade-off between environmental condition distribution (wind speed, turbulence intensity and number of samples) and the ability to analyse spectral responses at lower frequencies. Each chunk was processed to return environmental data, speed control performance, pitch actuator duty and structural loading metrics. Data was gathered with the LAC using feedback gains of 100%, 75%, 38% and 10% of Baseline gains (LAC100, LAC75, LAC38, and LAC10). A summary of data volumes is given in Table I and distributions according to wind speed and turbulence intensity are illustrated in Fig. 4. The analysis presented in this paper used more than 35 hours of data.

TABLE I. RECORDED DATA VOLUMES

Gains	Baseline 45-s Chunks	LAC 45-s Chunks
100%	137	110
75%	197	234
38%	54	43
10%	1423	614

Data from LAC100, LAC75 and LAC38 shows similar distributions and volumes to the baseline controller during their respective periods of operation, whereas LAC10 shows much lower levels of data collected compared to the baseline. Overall, the amount of data collected from LAC10 is still much greater than the other controller tunings.

A. Rotor Average Wind Speed Reconstruction Performance

The Avent LIDAR system is able to sample winds at multiple distances in front of the turbine. RAWS reconstructions taken closer to the turbine are likely to have a higher correlation to the "true" RAWS at the rotor plane. However, because the plane is closer, the sample points at the range gate are closer to the centre of the rotor, possibly losing data from spatial turbulence acting at the edge of the rotor. Using multiple gates can allow larger correlations while still maintaining adequate rotor coverage.

A wind speed estimator (WSE) was used to give the closest approximation to the "true" RAWS, which is used to test the coherence of RAWS estimated reconstructed from LIDAR signals. The estimator takes the following form:

$$V_{WSE|k+1} = AV_{WSE|k} + K(\alpha_{k+1} - \hat{\alpha}_{k+1})$$

where:

^ denotes an estimated value;

k is the time step index;

V_{WSE} is the wind speed estimate;

α is the rotor acceleration;

A is the state transition matrix; and

K is the estimator gain.

The linearised error dynamics of this estimator are defined by:

$$\Delta e_{k+1} = (A - KC)\Delta e_k$$

where:

$$e = \alpha_{k+1} - \hat{\alpha}_{k+1} ;$$

Given that in quasi-steady-state conditions the following relation is held:

$$P = \frac{1}{2}\rho A_r C_p(\omega, V, \theta)V^3$$

where:

P is the mechanical power from the rotor;

ρ is the air density;

A_r is the rotor area;

C_p is the power coefficient;

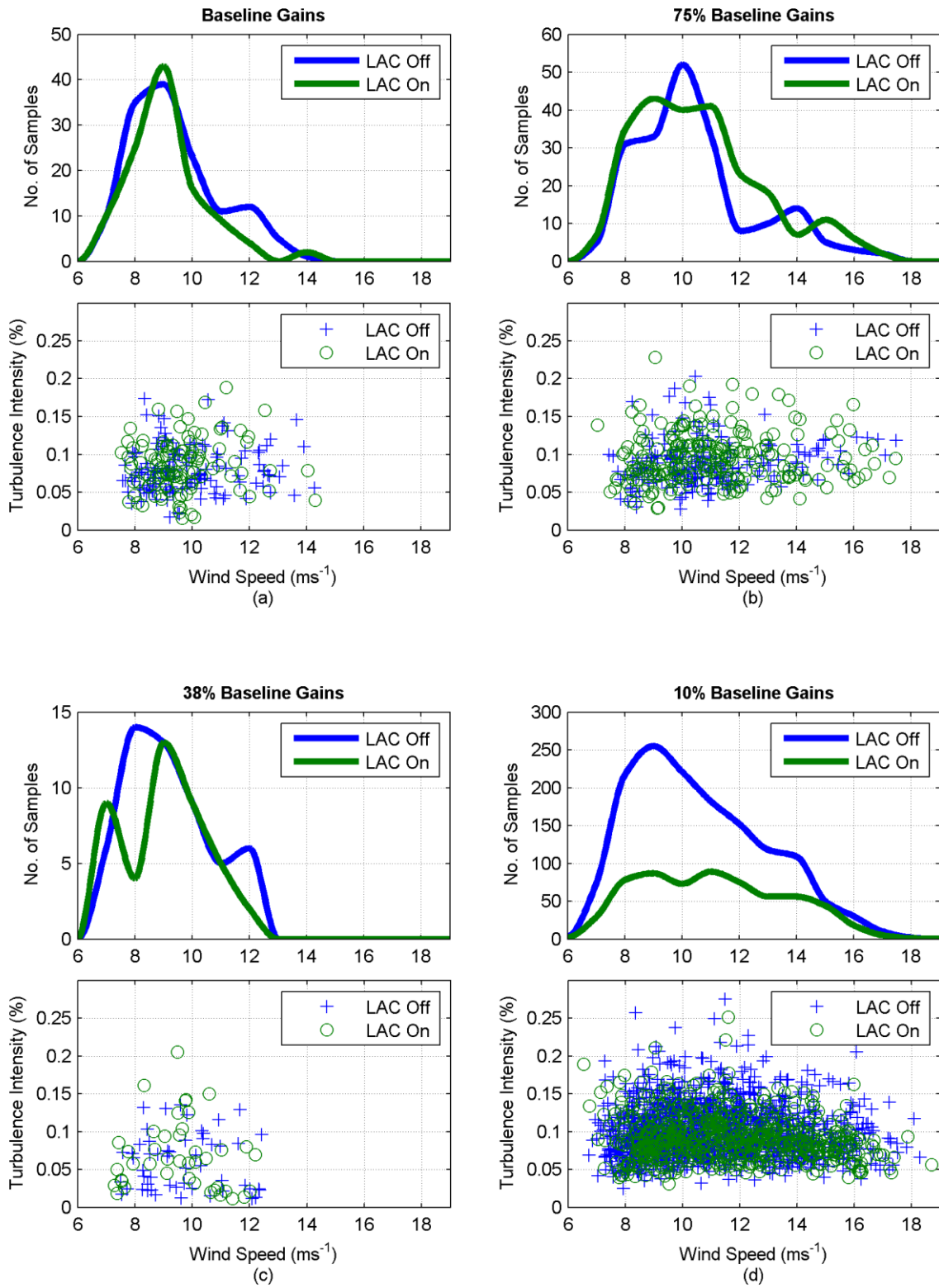ω is the rotor speed;

Figure 4.   Data wind speed distribution according to mean wind speed for each controller setting.
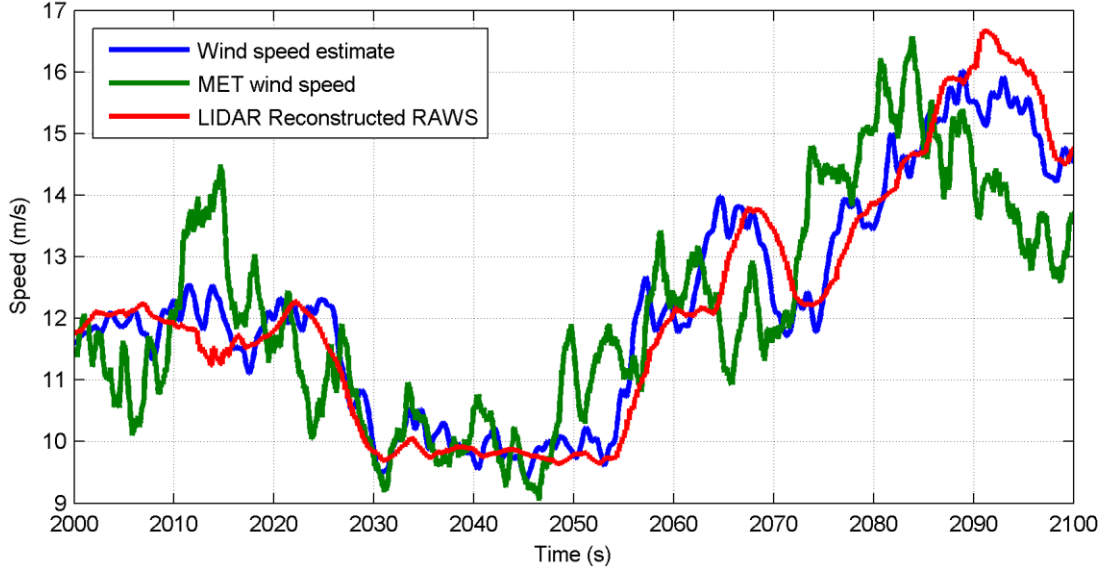
Figure 5.   Time series sample of meteorological mast wind speed measurement, V_{WSE} and V.

V is the rotor effective wind speed; and

θ is the mean blade pitch angle,

we get:

$$C = \frac{\partial \alpha}{\partial V} = \left(\frac{\rho A_r}{2 J_R \omega} \right)\left(\frac{\partial C_p(\omega, V, \theta)}{\partial V} V^3 + 3 C_p(\omega, V, \theta) V^2 \right)$$

By modelling the wind as a step input, A = 1, the estimator gain can be described in terms of an approximate time constant, τ, for the error dynamics:

$$K = \frac{1/\tau + 1}{C},$$

τ is set to 1 s for this study. C is recalculated online, allowing K to be updated each time step. In this realisation, the wind speed estimate is adjusted until the estimated and measured rotor accelerations match.

To find α, we differentiate and low-pass filter the measured rotor speed with time. The low-pass filter is a second-order, Butterworth filter with a natural frequency of 3 rads^{-1} and a damping ratio of 0.707.

To find $\hat{\alpha}$, we use the torque imbalance equation for a rigid drivetrain:

$$\hat{\alpha} = \frac{0.5 \rho A_r \mu C_p(\omega_k, V_{k-1}, \theta_k) V_{k-1}{}^3 - N Q_{g|k} \omega_k}{J_R \omega_k}$$

where:

Q_A is the aerodynamic torque;

Q_g is the generator torque;

N is the gearbox ratio;

μ is the drivetrain efficiency; and

J_R is the rotor inertia.

C_p can be found by interpolating over a lookup table of C_p as a function of pitch angle and tip-speed ratio. The resulting RAWS estimate, V_{WSE}, will show a lag relative to the "true" RAWS due to filtering. This lag will be similar to the lag from LIDAR-reconstructed RAWS signals because the latter is also filtered with a time constant of 1 s.

WSE outputs have been checked against meteorological (met) mast measured data and LIDAR reconstruction data; a time series sample is given in Fig. 5. The met mast is positioned 80 m away from the CART2 with an anemometer at the CART2's hub height (36.5 m). Due to the changing wind directions, the phasing between the RAWS and met mast measurements will be somewhat random, but the magnitude trends coincide very well. The LIDAR-reconstructed RAWS and the WSE reconstructions also coincide well, with slight phasing error.

Fig. 6 shows a magnitude squared coherence between $V_{WSE}(t)$ and $V(t)$ as reconstructed using data from each range gate individually and using data from all range gates together for a 200-minute data sample. The results demonstrate that combining data from all the gates results in the best performance, slightly outperforming data from Range Gate 1 above 0.1 Hz. The levels of coherence from Range Gate 1 are close to the combination of all range gates; this is likely due to the relatively large rotor coverage at a short focus distance, 63% and 50 m, respectively. As turbine sizes increase, we would expect a greater trade-off between LIDAR range and rotor scan area (assuming similar beam angles), amplifying the benefits of combining LIDAR measurements from multiple distances.
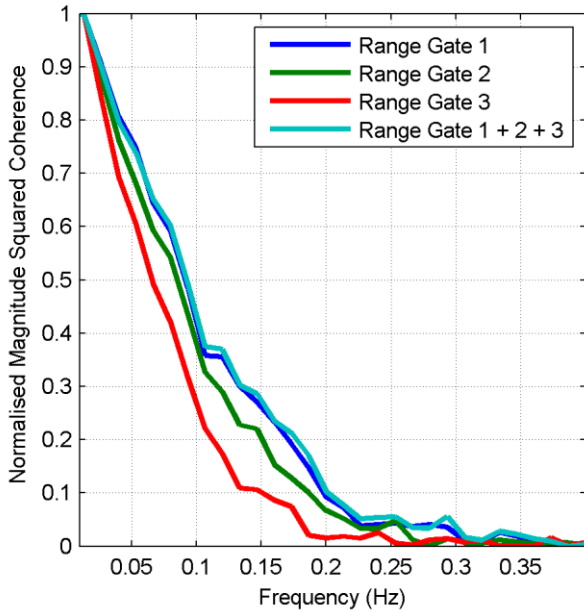
Figure 6. Magnitude squared coherence between $V_{WSE}(t)$ and $V_L(t)$ using different range gates.

B. Controller Performance

Rotor speed spectral response is the primary performance metric used in this study, chosen because the control algorithm is designed to assist the speed controller. The average normalised power spectral densities (PSDs) of the rotor speed for each controller are given in Fig. 7. LAC100 already shows a reduction in speed variance relative to the Baseline below 0.075 Hz, with a 19% reduction in peak spectral response (PSR). This frequency coincides with relatively high levels of coherence between the actual RAWS and the estimated RAWS (Fig. 5). Surprisingly, detuning to LAC75 actually shows a further reduction in relative rotor speed variance (64% reduction in PSR); this may indicate that the baseline gains are not necessarily optimal for rotor speed control on the de-rated turbine. Detuning further to LAC38 shows that the speed control performance begin to deteriorate — albeit slightly, at 58% reductions in PSR relative to the Baseline. The final detune to LAC10 shows that we have detuned enough for the speed control performance to fall and cause a 55% increase in PSR. Unfortunately, it was not possible to obtain a finer resolution of controller gains to determine the level at which speed control levels were at parity with the Baseline.

The reduction in controller gains from LAC100 to LAC10 resulted in decreasing levels of actuator usage beyond 0.1 Hz as expected (Fig. 8). Although overall levels of pitch rate activity fall dramatically beyond 0.1 Hz, the relative contribution of pitching at 1P (0.4 Hz), 2P and the tower first fore-aft modal frequency (0.87 Hz) is still relatively high until LAC38. In terms of speed control, it is a very positive result to see that the speed control performance of LAC75 and LAC38 outperforms

the baseline even though actuator usage levels have fallen.

The final piece of analysis of this campaign was to determine the impact of the reduced pitching levels on thrust-related fatigue damage. Fig. 9 shows the spectral response of the tower base fore-aft moment under different controller tunings. The results show that as the controller is detuned, the tower response between 0.13 Hz and 0.6 Hz shows less activity. However, the plots also show that the spectral response is dominated by activity at the tower natural frequency (0.87 Hz), which sits very close to 2P (0.8 Hz), with a much smaller peak at 1P. Fig. 7 (a)-(c) and Fig. 9 (a)-(c) show that the pitching around 1P and 2P for LAC100, LAC75 and LAC38 results in similar relative tower response levels at 1P and 2P despite the reduction in pitching away from these frequencies. LAC10, which showed very low levels of 1P and 2P pitching, shows much lower levels of 1P and 2P response levels relative to the Baseline (Fig. 9 (d)); however, the tower will be consistently excited at 2P because the CART2 is a two-bladed turbine.

Tower loading is further quantified in Fig. 10, which presents maximum, minimum and mean damage equivalent load (DEL) results for each operating condition and controller tuning. DELs were calculated using a rainflow counting algorithm with a 1-Hz cycle and an inverse S-N slopes of 4 [12]. Note that:

- The DEL comparisons have been taken with 45-s chunks, they do not include the lower end of the turbulence spectrum; and

- The wind conditions for each calculation have not been binned according to similar turbulence intensity levels.

With that in mind, LAC100 and LAC75 show no clear tower load reduction trends relative to the Baseline. LAC38 shows reductions in the 10-ms^{-1} and 11-ms^{-1} wind speed bins where a significant portion of data is collected, and an increase at 12 ms^{-1} where there is much less data. LAC10, on the other hand, shows a clear trend in the reduction of tower base DELs at all wind speeds above 8 ms^{-1} relative to the baseline. This indicates that the reduction in pitch actuation at 1P and 2P in addition to the general mid-high frequency pitching reductions have resulted in lower fatigue damage levels.

These results indicate that LAC can achieve comparable speed control with reduced levels of pitch activity. The reduction in pitch activity resulted in tower spectral response reductions, and if targeted correctly, these reductions can imply reductions in tower base DELs. Although the CART showed a strong tower response at 1P, 2P and tower first fore-aft frequency, turbines typically operate with a larger gap between rotor harmonics and structural frequencies, and controllers are typically tuned to avoid resonance at rotor harmonics, meaning that the relative impact on baseline loading levels from LAC could be much more significant on a more typical turbine.

IV. Conclusions

A field-testing campaign to test LAC has been undertaken on a 600-kW turbine using a fixed five-beam LIDAR system. The campaign compared the performance of a baseline controller relative to four LACs with progressively lower levels of feedback using 35 hours of collected data.

The collected data demonstrates that utilising measurements from multiple range gates on a pulsed LIDAR system can result in RAWS estimates with greater levels of correlation to wind speed at the rotor than using a single range gate. The benefits are likely to be more pronounced on implementations with larger rotors wherein each scanning range has a trade-off between distance and rotor coverage.

The LACs showed higher levels of speed control performance until controller gains had been reduced to 10% of baseline levels. The speed control was achieved with significantly reduced levels of pitch activity and generally lower levels of tower excitation.

LAC tower base DEL levels were consistently reduced relative to baseline levels once pitch activity at rotor harmonic frequencies and tower frequencies was sufficiently reduced (LAC10); however, at these controller gain levels, speed control performance was poorer than baseline levels. However, the CART2 loading spectrum was dominated by responses at 2P and the first tower fore-aft natural frequency, indicating that the response reduction is less significant for this turbine. The reduction is likely to be more significant with typical full-sized turbines, which show lower excitation levels due to harmonic clashes.

Acknowledgments

References

[1] E. A. Bossanyi, A. A. Kumar, and Hugues-Salas, "Assessment of Turbine Mounted LIDAR for Control Applications," in *EWEA*, 2012.

[2] D. Schlipf, E. Bossanyi, C. E. Carcangiu, T. Fischer, T. Maul, and M. Rossetti, "LIDAR assisted collective pitch control," UPWIND Deliverable D5.1.3Stuttgart, 2006.

[3] F. Dunne, L. Y. Pao, A. D. Wright, E. Simley, and B. Jonkman, "Adding Feedforward Blade Pitch Control for Load Mitigation in Wind Turbines: Non-Causal Series Expansion , Preview Control , and Optimized FIR Filter Methods," in *49th AIAA Aerospace Sciences Meeting*, 2011.

[4] J. Laks, L. Y. Pao, A. Wright, N. Kelley, and B. Jonkman, "Blade Pitch Control with Preview Wind," in *48th AIAA Aerospace Sciences Meeting*, 2010.

[5] D. Schlipf and P. Cheng, "Flatness-based feedforward control of wind turbines using Lidar," in *Proceedings of the 19th World Congress of the International Federation of Automatic Control*, 2014.

[6] L. C. Henriksen, "Model Predictive Control of Wind Turbines," Technical University of Denmark, 2012.

[7] A. A. Kumar, "Multivariable Control of Wind Turbines for Fatigue Load Reduction in the Presence of Nonlinearities," The University ofAuckland, Auckland, 2011.

[8] D. Schlipf, L. Y. Pao, and C. Po Wen, "Comparison of feedforward and model predictive control of wind turbines using LIDAR," in *Decision and Control (CDC), 2012 IEEE 51st Annual Conference on*, 2012, pp. 3050–3055.

[9] A. K. Scholbrock, P. A. Fleming, L. J. Fingersh, A. D. Wright, D. Schlipf, and F. Haizman, "Field Testing LIDAR Based Feed-Forward Controls on the NREL Controls Advanced Research Turbine Preprint," in *51st AIAA Aerospace Sciences Meeting*, 2013.

[10] D. Schlipf, P. Fleming, and F. Haizmann, "Field testing of feedforward collective pitch control on the CART2 using a nacelle-based lidar scanner," in *The Science of Making Torque from Wind*, 2012, vol. 2.

[11] P. A. Fleming, A. K. Scholbrock, A. Jehu, S. Davoust, E. Osler, a D. Wright, and A. Clifton, "Field-test results using a nacelle-mounted lidar for improving wind turbine power capture by reducing yaw misalignment," *J. Phys. Conf. Ser.*, vol. 524, Jun. 2014.
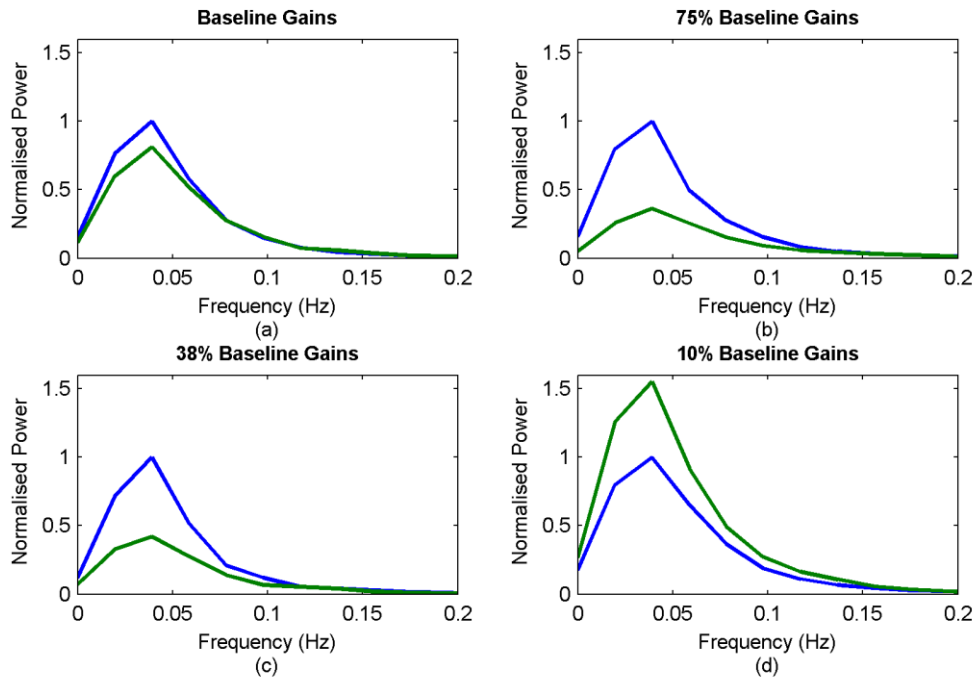
[12] DNVGL, *Bladed 4.5 User Manual*. 2013.

Figure 7.   PSD of rotor speed with different LAC tunings vs the Baseline controller binned by wind speed. Blue – Baseline, Green – LAC.
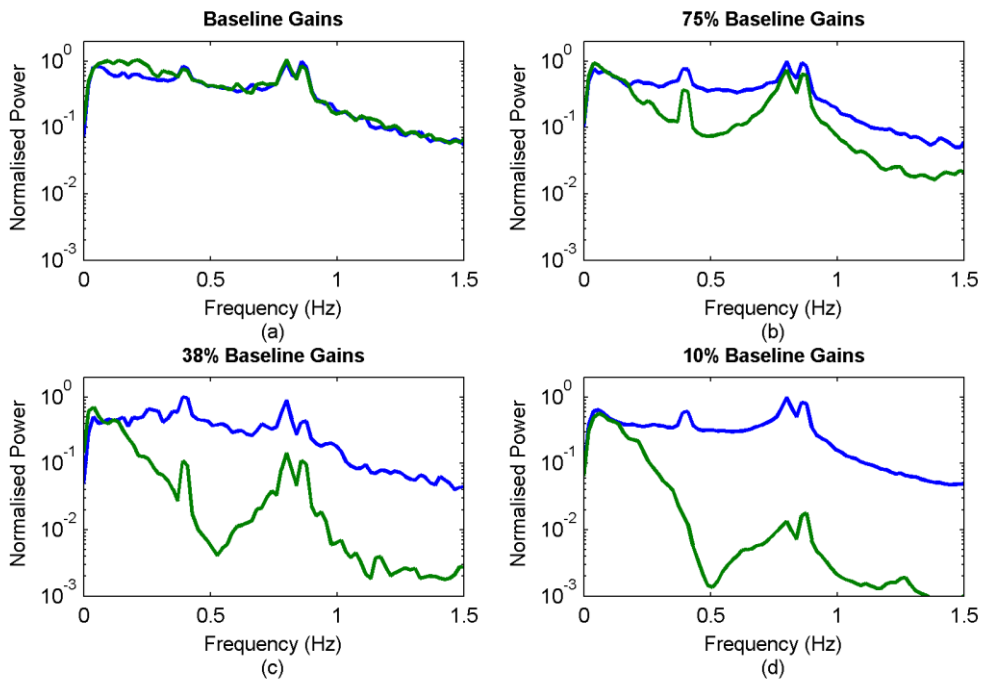

Figure 8.   PSD of pitch rate with different LAC tunings compared to the Baseline controller binned by wind speed. Blue: Baseline; Green: LAC.
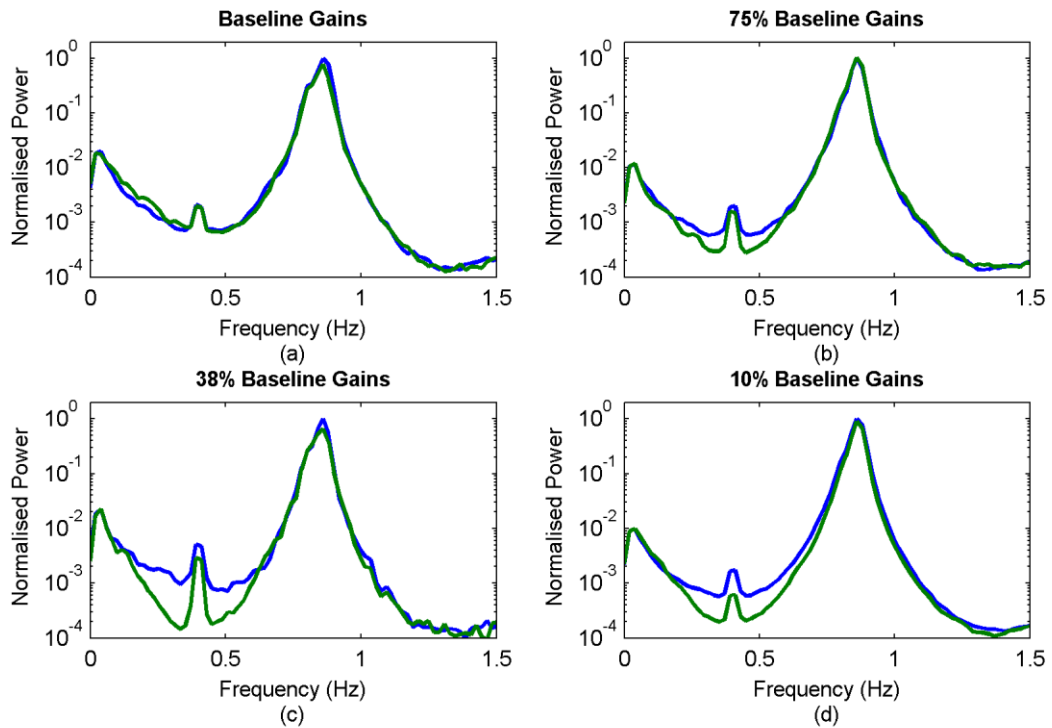
Figure 9.   PSD of tower base fore-aft moment with different LAC tunings compared to the Baseline controller binned by wind speed. Blue: Baseline; Green: LAC.
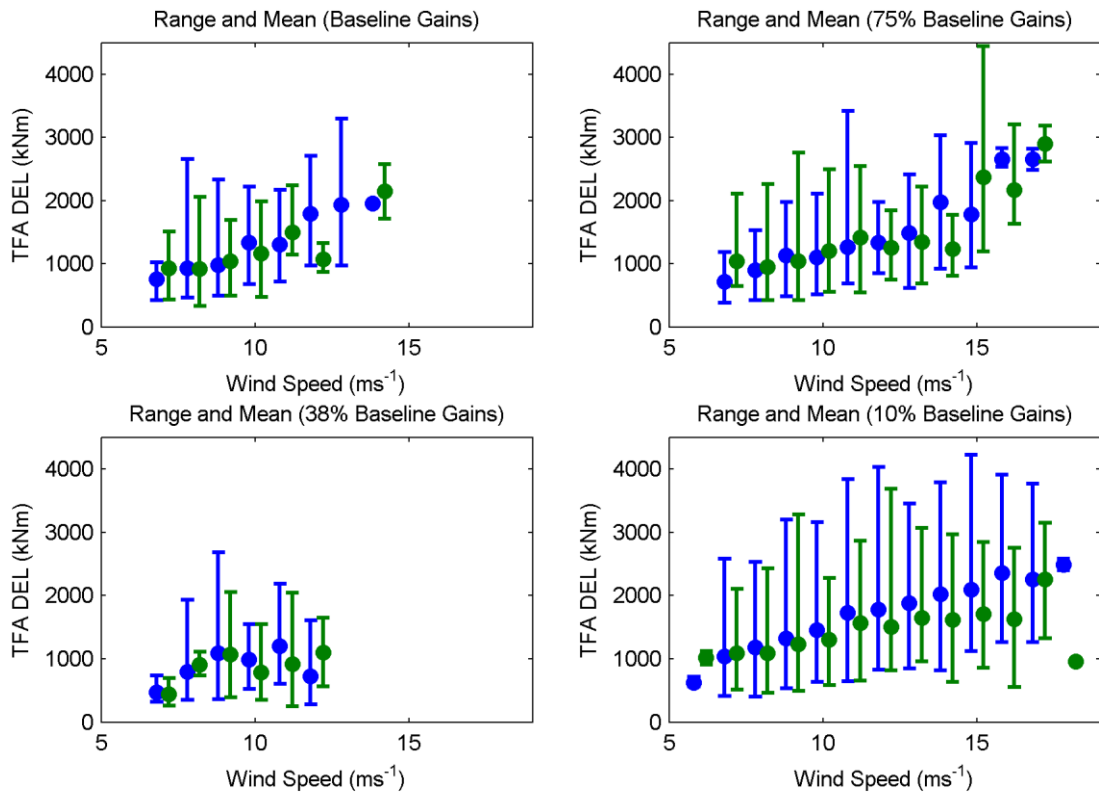

Figure 10. Tower base fore-aft DEL with different LAC tunings compared to the Baseline controller binned by wind speed. Markers indicate range and mean of data in each wind speed bin. Blue: Baseline; Green: LAC.